Trends in Sciences
TRENDS IN SCIENCES 2026; 23(10): 13375
DJMP Center for Digital Journal Management & Multidisciplinary Academic Platform
https://doi.org/10.48048/tis.2026.13375
RESEARCH ARTICLE

Anti-Premature Skin Aging Activities of Peptides from Black Soldier Fly (Hermetia illucens L.) Larvae: *In vitro* Analysis and Network Pharmacology

Sendy Junedi[1,*], Boy Rahardjo Sidharta[1], Agustina Setiawati[2] and Rudy Agung Nugroho[3]

[1]*Faculty of Biotechnology, Universitas Atma Jaya Yogyakarta, Yogyakarta 55281, Indonesia*
[2]*Faculty of Pharmacy, Sanata Dharma University, Yogyakarta 55284, Indonesia*
[3]*Animal Physiology, Development, and Molecular Laboratory, Department of Biology, Faculty of Mathematics and Natural Sciences, Mulawarman University, Kalimantan Timur 75123, Indonesia*

([*]Corresponding author's e-mail: sendy.junedi@uajy.ac.id)

Received: 17 January 2026, Revised: 25 March 2026, Accepted: 5 April 2026, Published: 25 April 2026

Abstract

Environmental factors and modern lifestyles contribute to premature skin aging, with an increasing number of young adults exhibiting it in subtropical and tropical regions. Bioactive peptides derived from *Hermetia illucens* L. larvae (black soldier fly larvae, BSFL) have been reported to exhibit antioxidant and antimicrobial activities; however, no study has comprehensively evaluated BSFL-derived peptides within a defined molecular weight range using an integrated in vitro and network pharmacology framework to address multiple mechanisms of premature skin aging. This study aims to extract, fractionate, and characterize peptides from BSFL, specifically targeting bioactivities relevant to premature skin aging in vitro. The peptides were isolated via alkaline solubilization and acid precipitation, followed by ultrafiltration, resulting in a peptide fraction with molecular weights of 3 to 30 kDa (PP). The bioactivities of PP were assessed using total antioxidant capacity, anti-tyrosinase, anti-collagenase, cytoprotection, and microbial modulation assays. Results indicated that the PP exhibited significantly enhanced antioxidant activity, tyrosinase inhibition, NIH/3T3 fibroblast proliferation, and protection of fibroblast from oxidative damage compared to crude protein extract (crude PP). Both PP and crude PP exhibited collagenase inhibition and microbial modulation activities against *Corynebacterium glutamicum*, a microbial genus model associated with skin aging, and *Staphylococcus epidermidis*, a beneficial bacterium found on skin. Among 261 tryptic peptides detected in PP by a bottom-up proteomic approach using LC-HRMS, 14 peptides were predicted to be biologically active by network pharmacology analysis. Network pharmacology analysis also predicted that the bioactive tryptic peptides target key proteins involved in skin aging, mainly MMP9, STAT3, and CASP3, which may support anti-collagenase and fibroblast proliferation assays. The results indicate that BSFL-derived peptides exhibit in vitro activities relevant to processes implicated in premature skin aging. These findings support further mechanistic validation in human cellular or tissue models to clarify their biological significance and potential application in skin-related formulations.

Keywords: Cytoprotection, *Hermetia illucens* larvae, Microbial modulation, Network pharmacology, Peptide, Skin aging

Introduction

Premature skin aging is a multifactorial process influenced by environmental stressors, notably ultraviolet (UV) radiation and pollution, as well as modern lifestyle factors [1,2]. These extrinsic insults, mainly UVB, accelerate the generation of reactive oxygen species (ROS), leading to oxidative stress and upregulation of matrix metalloproteinase (MMP)-1/collagenase, which degrade the extracellular matrix (ECM), such as collagen, and impair skin elasticity [3-5]. Protection of dermal fibroblasts from ROS is therefore crucial to preserve their viability and ECMproducing capacity. Oxidative stress in fibroblasts induces cell death, increases collagenase secretion, and decreases procollagen synthesis, whereas antioxidant treatments that lower intracellular ROS can reverse these effects and restore collagen production [6,7]. The ROS also activates melanocortin signaling, leading to increased tyrosinase expression and activity, consequently elevated melanin synthesis and hyperpigmentation characteristic of photo-aged skin [8,9]. Taken together, protecting dermal fibroblasts from oxidative stress while suppressing collagenase and tyrosinase activities is essential to maintain extracellular matrix integrity, prevent hyperpigmentation, and ultimately delay premature skin aging.

Emerging evidence highlights that skin microbiomes may contribute to skin homeostasis and aging. Several studies report aging-associated shifts in dominant genera i.e. *Corynebacterium* and *Streptococcus*, and reduced prevalence of *Staphylococcus* with site-, cohort- and method-dependent patterns [10-14]. This dysbiosis correlates with impaired hydration, altered pH, and reduced elasticity, thereby exacerbating aging phenotypes. Clinical trials have demonstrated that topical application of prebiotic and postbiotics ingredients can improve microbiome balance, reduce dysbiosis, and ameliorate aging signs such as wrinkles [15]. Peptides from animal sources (e.g., fish collagen) and plant sources (e.g., rice bran peptide KF-8) have been shown to modulate the microbiome in the wound skin and gut of animal models, respectively. This modulation involves increasing beneficial bacteria and decreasing harmful bacteria, which, in turn, contributes to improved skin wound healing and multiple aging-related phenotypes (including cognitive, muscular, and systemic inflammatory changes). These findings suggest that peptides may act as prebiotic/postbiotic-like agents that target the microbiome to support skin and aged conditions [16,17].

Based on epidemiological data from Queensland, Argentina, Singapore, and Malaysia, the burden of premature photoaging is very high, even in young adults, with up to 83% of individuals showing premature skin aging in subtropical Queensland, and about 28% of Argentine participants having a “skin age” older than their chronological age [18-20]. From a clinical and industrial perspective, the number of skin-aging clinical trials has risen sharply since around 2016, reflecting a rapid global expansion of anti-aging research [21,22]. At the same time, the recent systematic and narrative reviews emphasize persistent evidence gaps and the need for more effective and safe, including nutraceuticals, and cosmeceutical agents [21,23-25]. These data underscore a pressing, still-unmet need to develop safe, evidence-based, and mechanistically targeted anti-premature skin-aging agents capable of effectively mitigating the multiple mechanisms that induce aging.

Current anti-aging strategies are dominated by small molecules from plants that reduce ROS, inhibit MMPs, or modulate inflammation [26,27]. Compared to small molecules from plants, peptide-based anti-aging agents such as palmitoyl pentapeptide-4 and ginseng-derived peptides tend to have more specific molecular targets and multiple mechanisms of action, because they are designed or selected to interact with defined receptors and signaling pathways that regulate collagen synthesis, ECM remodeling, pigmentation, and inflammation, while often exhibiting high potency at low doses [28-31]. Nevertheless, to date, no research specifically addresses the effects of peptides on the modulation of the human skin microbiome during aging, an emerging strategy for maintaining skin homeostasis under aging conditions. Therefore, there remains a research gap for systematically identifying new peptides that, within a single experimental framework, protect fibroblasts from ROS, inhibit aging-related enzymes, and selectively modulate skin-associated bacteria, such as the *Corynebacterium* and *Staphylococcus*, to support skin health and delay aging.

The larvae of *Hermetia illucens* L. (Black Soldier Fly Larvae, BSFL) have gained increasing attention as a sustainable bioconversion agent for organic waste [32]. With a proximate composition of approximately 41% - 65% protein [33-35], BSFL represent an abundant bioresource of protein that may be valorized for higher-value applications. Proteins and peptides extracted from BSFL have demonstrated diverse biological activities, including antioxidant [36,37], antibacterial [38-41], anti-inflammatory [42], and wound-healing effects [43,44]. Most studies on protein and peptide BSFL focus on demonstrating the bioactivity of crude protein/hydrolysate rather than specific peptides or peptides with a size range. However, some studies have shown that protein hydrolysates with relatively high-molecular-weight peptide (≈ 14 - 25 kDa) exhibit strong antioxidant activity [37]. In contrast, antibacterial work has identified discrete short peptides from BSFL, i.e., defensin-like peptide 4 (40 amino acids, ~4 kDa) [41]. These reports indicate that BSFL proteins and peptides, specifically in the 3 - 30 kDa range, may be associated with their bioactivities. Despite this evidence, the application of these proteins and peptides in dermatology and skincare, particularly for anti-premature aging purposes, remains underexplored, and no peptide-based cosmetic formulations derived from *H. illucens* have yet been validated with strong scientific data.

The composition of bioactive peptides and proteins derived from BSFL remains largely unknown, and the specific target proteins of these bioactive peptides have not yet been clearly identified. Therefore, the bottom-up proteomics approach is applied for analyzing complex biological samples, in which proteins are enzymatically digested into peptides, separated by Liquid Chromatography (LC), and analyzed by high-resolution tandem MS (HRMS), followed by database searching for peptide and protein identification [45,46]. In this workflow, proteins are most commonly digested with trypsin, which cleaves at the carboxyl terminus of lysine and arginine residues, generating peptides of suitable length and charge-state distribution for LC-HRMS [47,48]. The resulting tryptic peptides typically bear multiple positive charges, a feature that enhances ionization efficiency in positive-mode electrospray ionization and yields fragmentation patterns favorable for reliable peptide identification [47,49]. The acquired MS/MS spectra are then matched to theoretical peptide spectra generated in silico from protein sequence databases, such as UniProt, using database search algorithms (e.g., a Sequest-type engine), enabling confident identification of the proteins and peptides present in the sample that contain tryptic peptide sequences [45,50]. The tryptic peptide data can then be used to determine which peptides are potentially bioactive through in silico prediction using relevant databases, such as PeptideRanker [51,52]. Subsequently, the predicted tryptic bioactive peptides are mapped to their potential skin-aging-related protein targets and analyzed using STRING-based protein-protein interaction (network pharmacology) to identify key target proteins of skin aging with the highest closeness and betweenness centrality [31,53]. This integrative approach is essential for pinpointing the critical protein targets of tryptic bioactive peptides from BSFL in skin aging and provides a rational foundation for subsequent mechanistic and therapeutic investigations.

This study aims to extract, fractionate, and characterize peptides from BSFL and to investigate their *in vitro* bioactivities relevant to premature skin aging. The novelty of this work lies in the comprehensive evaluation of BSFL-derived peptides within the 3 - 30 kDa molecular weight range, which has not previously been systematically investigated through an integrated assessment. Specifically, the study evaluates antioxidant activity, tyrosinase inhibition, collagenase inhibition, cytoprotective effects on fibroblast cells under oxidative stress, and microbial modulation, particularly in the genera *Corynebacterium* and *Staphylococcus*. To date, no research has comprehensively examined this peptide fraction for these combined anti-skin aging-related activities. Furthermore, the peptide composition was analyzed using LC-HRMS to identify potential bioactive peptides within the 3 - 30 kDa fraction, which have not previously been characterized in detail. The predicted bioactive peptides were subsequently subjected to network pharmacology analysis to identify their potential protein targets and protein-protein interaction networks associated with skin aging—an approach that has not been previously reported for BSFL-derived peptides. Overall, this study provides the first integrated experimental and in silico investigation linking BSFL-derived peptides in this molecular weight range to skin aging-related molecular pathways, thereby highlighting its scientific novelty and significance.

Materials and methods

Materials

Black Solider Fly egg, protein Quantification Kit (Bradford Assay), CheKine™ Micro Total Antioxidant Capacity (TAC) Assay Kit-product code KTB1500 (Abbkine Scientific Co., Ltd.), NaOH (Sigma-Aldrich), HCl (Sigma-Aldrich), NIH/3T3 fibroblast cells, DMEM (Dulbecco's Modified Eagle Medium) (Gibco), trypan blue (Gibco), fetal bovine serum (Gibco), Kalium Phosphate Buffer (Merck), Phosphate-Buffered Saline (Merck), penicillin-streptomycin (PAN), alcohol 70%, tripsin-EDTA (PAN), SuperKineTM Maximum Sensitivity Cell Counting Kit-8 (Abbkine Scientific Co., Ltd.), ProSieveTM QuadColor™ Protein Marker 4.6 - 300 kDa (Lonza), 4% - 15% Q-PAGETM TGN Precast Gel, distilled water, quercetin (Sigma-Aldrich), ascorbic acid (Sigma-Aldrich), Tyrosinase from mushroom lyophilized powder (Sigma MCLS), 3,4-Dihydroxy-L-phenylalanine (Sigma-Aldrich), kojic acid (Sigma-Aldrich), Collagenase Activity Assay Kit-product code ab196999 (Abcam), Amicon 30 kDa MWCO (Merck), Amicon 3 kDa MWCO (Merck), *Staphylococcus epidermidis*, *Corynebacterium glutamicum*, Tryptic Soy Broth (Oxoid), Tryptic Soy Agar (Merck).

BSFL rearing

Eggs from the black soldier fly were sourced from a local supplier, CV. Ahasa Larva Group, located in Samarinda, East Kalimantan, Indonesia. After a 4-day incubation period, the eggs hatched into young larvae. These larvae were then placed in a controlled setting inside a plastic container, where the temperature was kept at 28 °C, and humidity was maintained 60% - 70%. Over the next 7 days, the larvae were fed standard chicken feed pellets to support their initial growth and development [54].

The main substrate used for larval cultivation was palm kernel meal (PKM), sourced from REA Kaltim Plantation, Ltd., in East Kalimantan, Indonesia, and fermented to improve its effectiveness. This process involved mixing 180 g of molasses, 279 mL of effective microorganism 4 (EM4) solution, 2.5 L of water, and 2.5 kg of PKM. The mixture was sealed in a plastic bag and left to ferment undisturbed at room temperature. A 5% fructose concentration was found to be optimal for larval development and nutritional quality. For the rearing environment, 5 rectangular plastic containers, each measuring 24 cm in length, 15 cm in width, and 6 cm in height, were used. Each container housed 200 larvae that were 7 days old, with the experiment being repeated 3 times, resulting in a total of 3,000 larvae. Humidity was maintained at 60% - 70% by adding water to the substrate as necessary, while the ambient temperature was kept constant at 28 °C. Feeding amounts were adjusted based on protocols from previous studies to ensure proper nutrition. The rearing process continued until about 90% of the larvae reached the prepupal stage, by day 22, at which point they were collected for further processing [54,55].

Preparation of defatted BSFL

Once the larvae reached the prepupal stage, they were thoroughly washed with water and then quickly dipped in hot water for approximately 30 s to ensure sanitation. They were subsequently dried in an oven at 60 °C for 24 h. After drying, the specimens were subjected to an oil extraction press to separate the defatted meal from the lipid content, making them ready for further analytical evaluations [54,56].

Extraction and separation of peptides

Crude protein and peptide (crude PP) extraction was performed according to the procedure of Xu *et al.* [57] with modifications. Defatted BSFL powder was ground and sieved, then mixed with 0.4 M NaOH at a ratio of 1:15, then heated at 40 °C with shaking at 200 rpm for 60 min, followed by centrifugation at 5,000×g, 4 °C for 20 min. The supernatant was collected and adjusted to pH 4.3 - 4.5 with 2 M HCl to precipitate proteins. The protein precipitate was obtained by centrifugation at 12,000×g, 4 °C for 20 min, washed with distilled water until the pH of the distilled water approached 7, and then freeze-dried. Ultrafiltration was carried out as described by Maron *et al.* [52], with modifications. Crude PP powder was dissolved in 20 mM potassium phosphate buffer (pH 7.4), filtered using a 0.22 µm filter, placed in an Amicon 30 kDa MWCO, and centrifuged at 2,500×g, 4 °C, for 20 min. The < 30 kDa protein-peptide fraction was put into an Amicon 3 kDa MWCO device to obtain the 3 - 30 kDa proteins and peptides fraction (PP). Crude PP, which contains all proteins and peptides (< 30 and ≥ 30 kDa), together with PP, was stored at −20 °C for further analysis. Protein concentration was determined using the Bradford assay. Protein profile and molecular weight were analyzed by 4% - 15% SDS-PAGE.

Determination of total antioxidant capacity

Total antioxidant capacity was determined using the CheKine™ Micro Total Antioxidant Capacity (TAC) Assay Kit. Ten µL of 100 µg/mL ascorbic acid as a positive control or 300 µg/mL PP/crude PP was added to 180 µL Fe^{3+}-tripyridine triazine in acidic solution, incubated at room temperature for 5 min, and the absorbance of blue Fe2+-tripyridine triazine was measured at a wavelength of 593 nm using a microplate reader. TAC values of samples and positive control were calculated according to the Fe^{2+} standard curve and expressed as µmol/mL. All experiments were carried out independently 3 times.

Anti-tyrosinase assay

Tyrosinase inhibition activity was assessed according to method of Namjoyan *et al.* [58] with some modification. In brief, 50 µL of mushroom tyrosinase (250 U/mL), 25 µL of 50 mM potassium phosphate buffer pH 6.5 (KPB), and 50 µL of either PP/crude PP (300 µg/mL) or kojic acid as positive control (50 µg/mL) were mixed and incubated at 37 °C for 10 min. Then, 50 µL of 7.6 mM L-DOPA in KPB was added, and the mixture was incubated again at 37 °C for 15 min. Absorbance of dopachrome formation was measured at a wavelength of 475 nm using a microplate reader, and tyrosinase inhibition activity (%) was calculated as below. All experiments were carried out independently 3 times.

$$\%\ \text{tyrosinase inhibition} = \frac{(A - B) - (C - D)}{(A - B)} \times 100\% \qquad (1)$$

where, A = absorbance of tyrosinase and L-DOPA mixture; B = absorbance of KPB and L-DOPA mixture; C = absorbance of tyrosinase and L-DOPA mixture in the presence of PP/crude PP/ kojic acid (samples); D = absorbance of samples and L-DOPA mixture.

Anti-collagenase assay

Anticollagenase assay was performed using the Collagenase Activity Assay Kit (Colorimetric). This assay measures collagenase activity using a synthetic peptide (FALGPA) that mimics the structure of collagen. Ten µL of PP or crude PP (300 and 600 µg/mL) were mixed with 10 µL of collagenase and 80 µL of buffer. A positive control contained 1,10-phenanthroline as a pure inhibitor, whereas the negative control contained only the enzyme and the buffer. The reaction was started by adding 40 µL of FALGPA (substrate) and 60 µL of substrate buffer. Absorbance was measured at a wavelength of 345 nm on a microplate reader in kinetic mode for 15 min at 37 °C protected from light. Collagenase activity and collagenase inhibition (%) were calculated as below. All experiments were carried out independently 3 times.

$$\text{Collagenase activity (U/mL)} = \frac{\{[-(\Delta A345/\Delta T)\text{sample }] - [-(\Delta A345/\Delta T)\text{ blank}]\}\times RV\times D}{0.53\times V} \qquad (2)$$

where, ΔA345 = Δ absorbance at T2 =15 min and T1= 0 min; ΔT = linear phase reaction time 15 min – 0 min = 15 min; RV = reaction volume = 0.2 mL; D = sample dilution factor = 1; 0.53 = millimolar extinction coefficient of FALGPA; V = sample volume added into the reaction well = 0.01 mL.

$$\%\ \text{collagenase inhibition} = \frac{A - B}{A} \times 100\% \qquad (3)$$

where, A = collagenase activity without inhibitor; B = collagenase activity in the presence of PP/crude PP /1,10-phenanthroline as inhibitor.

Fibroblast proliferation and protection assays

Fibroblast proliferation assay was performed based on method of Sen *et al.* [59] with some modifications. NIH/3T3 fibroblast cells (8,000 cells/well) were seeded in DMEM supplemented with 10% FBS and 1% PenStrep for 24 h at 37 °C, 5% CO_2. Cells were then pre-treated with serial concentrations of crude PP or PP in DMEM containing 0.5% FBS and 1% PenStrep for 24 and 48 h under the same conditions. Cell numbers after incubation were measured using the WST assay, and the percentage of the control (cells without sample treatment) was calculated.

For the fibroblast protection analysis, NIH/3T3 fibroblast cells (8,000 cells/well) were seeded in DMEM supplemented with 10% FBS and 1% PenStrep for 24 h at 37 °C, 5% CO_2. Cells were then pre-treated with 2 concentrations of crude PP or PP in DMEM containing 0.5% FBS and 1% PenStrep for 24 h under the same conditions. For oxidative stress conditions, 400 µM H_2O_2 was added to the cell culture and incubated for 24 h without or with crude PP or PP, followed by the WST assay. Cell numbers after incubation were determined using the WST assay by measuring absorbance at 450 nm, and cell viability was calculated relative to the control (cells without sample treatment).

Microbial modulation analysis

Microbial modulation analysis was conducted according to method of Ardalani *et al.* [60] with some modifications. The microorganisms used in this study were obtained from Center for Food and Nutrition/ Pusat Studi Pangan dan Gizi, Universitas Gadjah Mada, Yogyakarta, Indonesia, and authenticated by the same institution as stated in the official certificate of microbial identification. *Staphylococcus epidermidis*, strain number: FNCC 0048, certificate no FNCC-PSPG/232/VI/2025, and *Corynebacterium glutamicum*, strain number: FNCC 0062, certificate no FNCC-PSPG/234/VI/2025. Both microorganisms were cultured in Tryptic Soy Broth (TSB) until OD600 ~0.10 - 0.15 (observed by microplate reader). For single culture assays, 20 µL of bacterial suspension was added to 96-well plates, followed by 160 µL TSB, 20 µL of crude PP or PP, incubated at 37 °C for 24 h, and growth was measured at OD600. For co-culture assays, the 2 bacteria were combined at a 1:1 ratio, i.e., each 10 µL, treated without (cell control) or with 20 µL crude PP or PP, and then 160 µL TSB was added to 96-well plates. Cells were incubated at 37 °C for 24 h. The cells were detected at OD600, and the percentage of cell number was calculated relative to the control (cells without sample treatment).

$$\%\ \text{cell number} = \frac{\text{OD600sample} - \text{OD600medium}}{\text{OD600cell control} - \text{OD600medium}} \times 100\% \tag{4}$$

OD600sample = absorbance of cells after being treated with the sample for 24 h
OD600cell control = absorbance of cells without treatment
OD600medium = absorbance of medium as blank

Peptides identification using bottom-up proteomic approach

Amino acid composition and sequence of PP were analyzed by liquid chromatography (Thermo Scientific™ Vanquish™ UHPLC Binary Pump) and Orbitrap high-resolution mass spectrometry (Thermo Scientific™ Q Exactive™ Hybrid Quadrupole-Orbitrap™ High Resolution Mass Spectrometer). The PP sample was prepared by adding 200 µL of 50 mM ammonium bicarbonate (pH 8.0) to 50 µL of PP. Following the addition of 10 µL of 10 mM dithiothreitol (DTT) and then incubation at 56 °C for 60 min. Ten µL of 20 mM Iodoacetamide (IAA) was added to the sample solution, incubated in the dark for 60 min. Ten µL of 0.1 mg/mLPierce Trypsin Protease MS grade (Thermo Fisher) was added, then incubated at 37 °C for 17 h. The sample was diluted with 500 µL of 1% TFA (Merck), followed by filtration through a 0.2 µm PVDF filter, and then 5 µL was ready to be injected into the LC-HRMS machine.

Liquid chromatography was carried out using an analytical column of Thermo Scientific™ Acclaim™ PepMap™100 C18 150 mm length×1 mm ID × 3 µm. The mobile phases used were MS-grade water containing 0.1% formic acid (A) and MS-grade acetonitrile containing 0.1% formic acid (B) employing a gradient technique with the flow rate of 75 µL/min. The mobile phase condition was as follows: 0 - 1 min (5% B), then 1 - 31 min, the mobile phase of B was gradually increased from 5% to 50%, and held for 2 min. After that, the mobile phase was set to 90% B for 2 min, then to 5% B for 45 min. The column temperature was set to 30 °C. The untargeted screening was carried out using full MS/dd-MS2 acquisition mode at positive ionization mode. Nitrogen was used for sheath, auxiliary, and sweep gases, and they were set at 10, 5, and 1 arbitrary units (AU). The spray voltage was 4.00 kV, and the capillary temperature was set at 300 °C. The scan range was performed at 350 - 1,500 m/z, and the resolution used was 120,000 for full MS and 15,000 for dd-MS2. Data was analyzed with Thermo Scientific™ Proteome Discoverer™ 2.5 (San Jose, CA, USA), SequestHT (University of Washington), and UniProt (European Molecular Biology Laboratory Incorporated Association) database.

Network pharmacology analysis: Target prediction and collection

The PeptideRanker server (http://distilldeep.ucd.ie/PeptideRanker/) was used for the prediction of bioactive peptides from PP, which can score the probability of different peptides to be biologically active in the range of 0 (worst activity) to 1 (highest predicted activity). The Similarity Ensemble Approach (SEA) (https://sea16.docking.org/) was used to predict and screen potential targets associated with bioactive peptides in PP. Skin aging-related targets were obtained from GeneCards (https://www.genecards.org/) using the keywords "skin aging" OR "dysbiosis" (Skin Aging). A Venn diagram and Cytoscape were used to show the network of related targets of peptides and Skin Aging (SA).

Network pharmacology analysis: GO analysis, construction of protein-protein interaction (PPI) network, and target screening

Various mechanisms of bioactive peptide action on SA were further studied through GO enrichment analysis from the DAVID database (https://david bioinformatics.nih.gov/). The GO biological process (BP), cellular composition (CC), and molecular function (MF) data were input to SRPlot (https://bioinformati cs.com.cn/) to get an enrichment dot bubble diagram. The targets of predicted bioactive peptides from PP related to SA were entered into STRING (https://string-db.org/) for protein interaction analysis, and a score ≥ 0.40 was set to obtain a protein-protein interaction network, which was subsequently plotted using Cytoscape. The degree values of each target were calculated using Analyze Network, and the target pathway networks were considered as potential targets.

Statistical analysis

All *in vitro* bioactivities data were presented as mean ± standard deviation (n = 3). The data were analyzed using one-way analysis of variance (ANOVA) to assess the statistical significance of differences among samples ($p < 0.05$). Duncan's multiple range test ($\alpha = 0.05$) was employed to identify significant differences among groups. Statistical analysis was conducted using SPSS® software version 15.0 (SPSS Inc., Chicago, IL, USA).

Results and discussion

Extraction of proteins and peptides

Extraction of protein and peptide from BSFL powder was carried out using an alkaline solubilization method at pH 13.9, followed by acid precipitation. Acid precipitation was performed until the pH reached 4.3 - 4.5, resulting in protein and peptide precipitates, which were then washed with distilled water to remove residual acids and salts. After freeze-drying, the extracted material yielded a dry crude PP powder with a recovery of 7.5% (w/w). Protein extraction using alkaline solubilization and acid precipitation is a commonly applied method for isolating proteins and peptides from BSFL at different developmental stages [61]. In alkaline conditions, non-covalent interactions (such as hydrogen bonds and hydrophobic interactions) and disulfide bonds are disrupted, promoting protein unfolding and exposing more hydrophilic regions. Moreover, the carboxyl groups on amino acids deprotonate, giving proteins a strong negative charge, which further increases their solubility [62]. When HCl is added to lower the pH to 4.3 - 4.5, the pH approaches the isoelectric point (pI) of the proteins from BSFL. At the PI, the number of positive and negative charges on the protein surface is balanced, resulting in a net charge of zero. This neutral charge minimizes electrostatic repulsion between protein molecules, causing them to aggregate and become insoluble, resulting in precipitation [63,64].

Separation and identification of peptides

To obtain PP in the 3 - 30 kDa range, ultrafiltration was performed using a 30 kDa MWCO (molecular weight cut-off) membrane followed by a 3 kDa MWCO membrane. The size distribution of ultrafiltrated PP was confirmed by SDS-PAGE (**Figure 1**) and compared with crude PP. The results showed that ultrafiltered PP predominantly ranged from 4.6 to 10 kDa, while crude PP contained proteins and peptides ranging from 4.6 to 300 kDa, indicating that ultrafiltration successfully separated lower-molecular-weight (PP) from Crude PP. As mentioned in some previous references, the molecular weight of peptides typically ranges from about 200 up to 5,000 - 10,000 Da. Molecules above this range are generally classified as proteins [65,66].

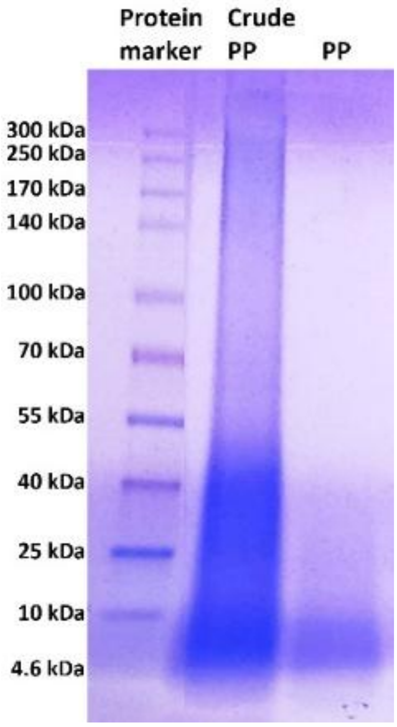

Figure 1 SDS-PAGE result of crude PP after extraction, dan PP after ultrafiltration of crude PP.

Total antioxidant capacity

The antioxidant capacity of crude PP and PP was evaluated by measuring their ability to reduce oxidizing agents, expressed as Total Antioxidant Capacity (TAC). The FRAP assay used in this study is an electron-transfer-based method. It measures the ability of antioxidants to donate electrons, reducing Fe^{3+} to Fe^{2+}. Higher reducing power corresponds to higher TAC values, reflecting one mechanism by which antioxidants inhibit oxidation reactions. Results showed that PP exhibited significantly higher TAC values than crude PP at the same concentration (**Figure 2(A)**). The PP contains peptides and proteins within the 3 - 30 kDa range, whereas crude PP contains peptides and proteins < 30 kDa as well as proteins ≥ 30 kDa. The higher total antioxidant capacity (TAC) observed in PP compared to crude PP suggests that removing proteins ≥ 30 kDa may contribute to the enhanced antioxidant activity. These findings indicate that higher-molecular-weight proteins (≥ 30 kDa) may dilute or reduce the measurable antioxidant effect, although further fractionation studies are required to confirm their specific contribution. In previous reports, peptides typically less than 10 kDa are more effective antioxidants because they can more easily interact with and neutralize free radicals and have greater accessibility to target molecules than larger proteins or peptides [67,68]. Previous study reported that peptides in the 3 - 10 kDa range from BSFL had the best antioxidant activity, especially those rich in aromatic (e.g., tryptophan, tyrosine, phenylalanine) and hydrophobic amino acids [67]. This result highlights that size is a crucial parameter for determining antioxidant capacity, along with amino acid composition.

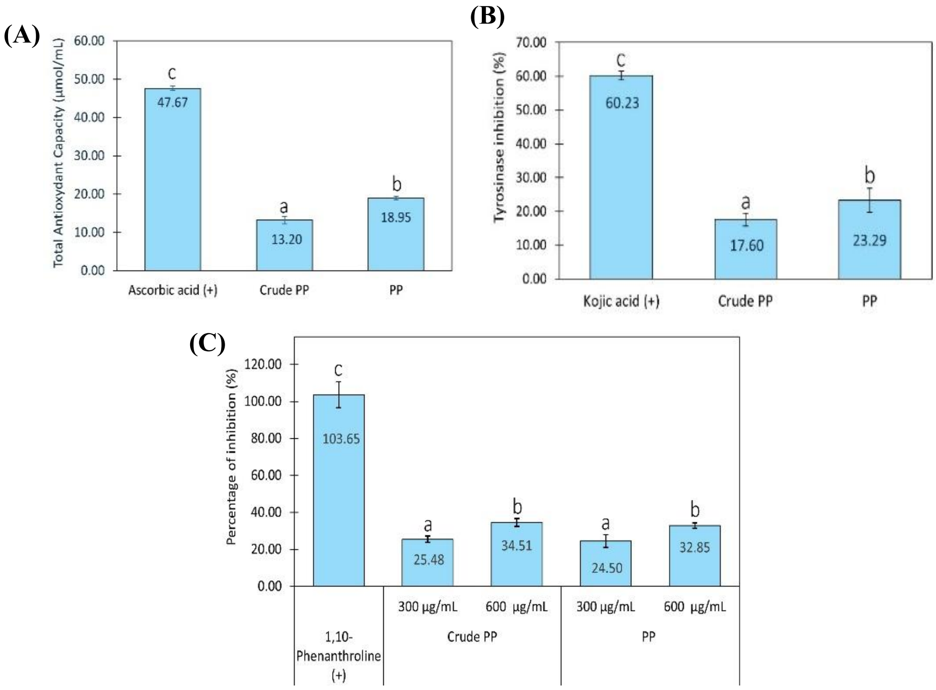

Figure 2 Total antioxidant capacity (A), tyrosinase inhibition (B), and collagenase inhibition (C) by crude PP and PP. (+) indicates pure compounds, namely ascorbic acid, kojic acid, and 1,10-phenanthroline used as positive controls in each analysis. Concentration of crude PP and PP in TAC and anti-tyrosinase assays was 300 µg/mL. Graph data are expressed as the mean of 3 replicates ± SD. Bar chart with different letter markers indicating significant differences ($p < 0.05$).

Anti-tyrosinase and anti-collagenase analysis

Antioxidants are known to inhibit the oxidation of L-DOPA into dopaquinone, a reaction catalyzed by tyrosinase. This inhibition may occur through several mechanisms, including direct enzyme inhibition, reduction of o-quinones, or chelation of metal ions at the enzyme's active site [69-71]. Dopaquinone is an intermediate in melanin biosynthesis and contributes to hyperpigmentation, a hallmark of premature skin aging [72]. Oxidative stress also contributes to upregulating collagenase expression, leading to collagen degradation in the skin's dermal layer, a sign of skin aging. Antioxidants reduce oxidative stress, thereby indirectly suppressing collagenase activity [73]. Some antioxidants directly bind to collagenase, inhibiting its function [74,75].

In this study, crude PP and PP were analyzed for their ability to directly inhibit tyrosinase and collagenase. PP exhibited stronger inhibition of mushroom tyrosinase activity compared with crude PP with the same concentration (**Figure 2(B)**). Whereas in the anti-collagenase assay, both crude PP and PP have the same activity to inhibit collagenase activity (**Figure 2(C)**). These results indicated that PP has more effective direct inhibition of tyrosinase than crude PP. The direct inhibition might be related to the binding of peptides in PP with tyrosinase, which inhibits its active site. On the other hand, protein and peptide in crude PP, and peptide in PP, exhibited the same ability to directly bind and inhibit collagenase.

Multiple recent studies using in vitro assays and molecular docking analyses have demonstrated that tyrosinase inhibitory peptides primarily exert their effect by binding to the enzyme's active site. Peptides with hydrophobic or aromatic residues often show strong binding and inhibition due to their ability to interact with critical residues in tyrosinase and/or chelate copper ions at the catalytic center of tyrosinase [76-78]. Molecular docking and simulation studies also demonstrate that various bioactive peptides from natural sources (e.g., whey, chia seed, and cricket) can bind to the collagenase active site, forming hydrogen bonds and hydrophobic interactions with catalytic residues. This binding often mimics the substrate, thereby inhibiting collagenase activity and preventing its breakdown [79-81].

Fibroblast proliferation and cytoprotection analysis

In addition to inhibiting tyrosinase activity in oxidation reactions, antioxidants may also neutralize free radicals that suppress fibroblast proliferation in the dermis, a key factor in the premature aging of skin [82]. In this study, the NIH/3T3 mouse fibroblast cell line was used because it is a well-established and robust in vitro model widely used to study oxidative stress, cytotoxicity, and the cytoprotective effects of bioactive compounds, including antioxidant peptides, prior to validation in primary human cells in future studies [83-85]. Fibroblasts treated with reactive oxygen species (ROS), specifically 400 µM hydrogen peroxide for 24 h, showed about 40% reduction in cell number compared to untreated controls (**Figure 3**). This demonstrates that ROS reduces fibroblast viability, making it a suitable model for fibroblast decline under premature-aging conditions. In this study, PP or crude PP was administered to ibroblasts for 24 h prior to hydrogen peroxide treatment, followed by continued exposure to hydrogen peroxide and PP or crude PP for an additional 24 h. After 48 h, the cell number after PP treatment was higher than that of cells with or without hydrogen peroxide exposure. In contrast, the cell number after crude PP treatment was similar to that of cells treated with hydrogen peroxide (**Figure 3**). These findings indicated that PP protects fibroblasts from ROS-induced damage.

Furthermore, when fibroblasts were treated with PP or crude PP without ROS exposure, different effects were observed. Fibroblast proliferation increased in a concentration-dependent manner with PP, whereas crude PP neither enhanced proliferation nor induced cytotoxicity after 24 and 48 h (**Figure 4**). These results suggest that both PP and crude PP are non-toxic and safe for fibroblasts. Evidence from diverse peptide sources indicates that concentrations around 250 - 300 µg/mL fall within an effective and non-toxic range for antioxidant, anti-aging enzyme inhibition, anti-inflammatory, antimicrobial, and cytoprotective activities in vitro [86,87]. Therefore, the concentration of 300 µg/mL used in this study can be considered biologically relevant within the experimental framework of peptide-based skin research. Importantly, since PP increases cell number in the absence of oxidative stress (**Figure 4**), the observed protection in **Figure 3** may involve both cytoprotective and pro-proliferative mechanisms. Direct ROS assays in human fibroblasts are required in the future to attribute the effect specifically to antioxidant activity in cells. In addition, further studies evaluating the ability of PP to enhance collagen synthesis and inhibit MMP expression in human fibroblasts are necessary to substantiate its claim as an anti-premature aging material.

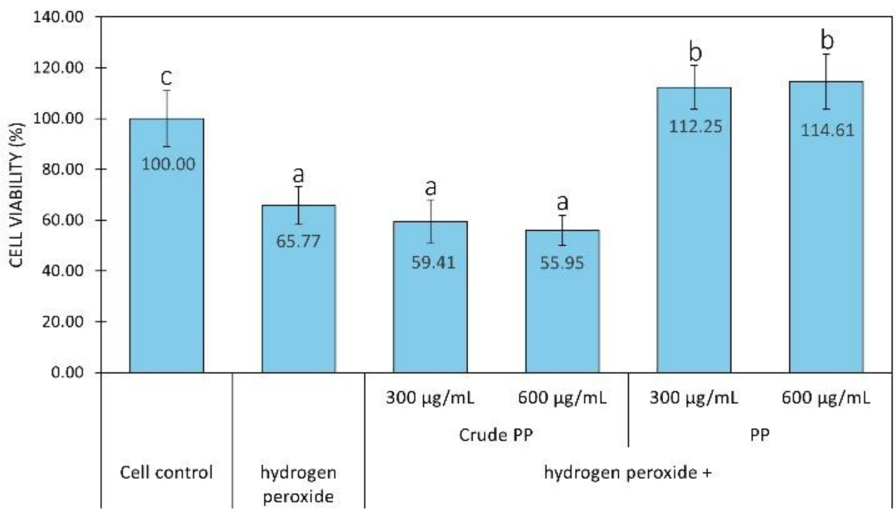

Figure 3 Fibroblast cell viability after hydrogen peroxide treatment with or without crude PP and PP. Graph data are expressed as the mean of 3 replicates ± SD. Bar chart with different letter markers indicating significant differences ($p < 0.05$).

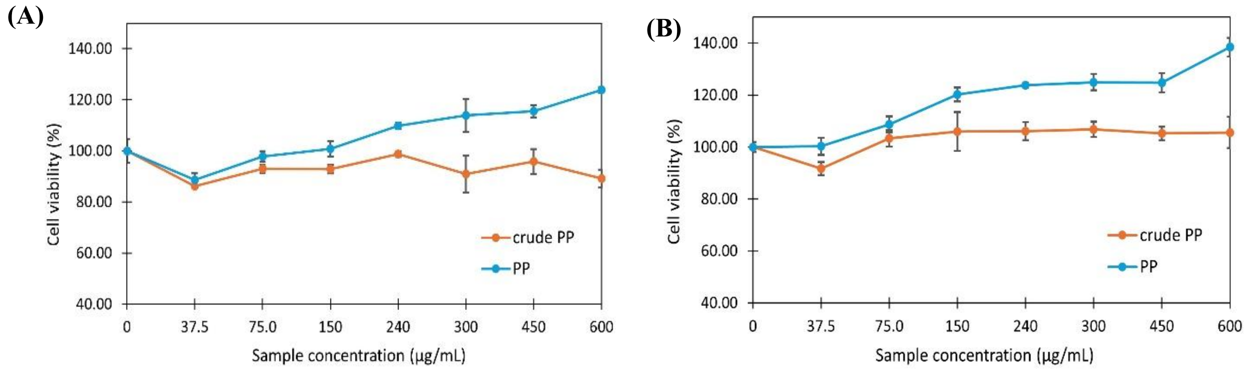

Figure 4 Fibroblast cell viability after treatment with crude PP and PP for 24 h (A) and 48 h (B). Graph data are expressed as the mean of 3 replicates ± SD.

Microbial modulation

Skin aging is often accompanied by microbial imbalance (dysbiosis), which affects skin hydration and pH. Aged skin is typically dominated by *Corynebacterium* genus and shows reduced levels of *Staphylococcus* genus [10-12]. In this study, *S. epidermidis* and *C. glutamicum* were used as skin microbiome models to assess the effects of PP and crude PP on *Corynebacterium* and *Staphylococcus* genera under monoculture and co-culture (1:1) conditions. At 300 µg/mL, PP significantly reduced *C. glutamicum* compared to crude PP, while at 600 µg/mL, both PP and crude PP significantly suppressed *C. glutamicum* (**Figure 5**). For *S. epidermidis*, PP (300 and 600 µg/mL) had no effect on cell numbers, whereas crude PP (300 and 600 µg/mL) significantly increased *S. epidermidis*. In co-culture conditions, PP showed no effect, but crude PP increased total cell counts (**Figure 5**). The effects of PP and crude PP (600 µg/mL) on cell numbers in co-culture and monoculture of *S. epidermidis* were similar. The results of this study indicate that crude PP modulates both *S. epidermidis* and *C. glutamicum*, whereas PP selectively modulates *C. glutamicum* under the tested conditions. Our findings suggested that BSFL-derived peptides may act as microbial modulators that need to be validated in a human study.

It is important to note that *C. glutamicum* is not a classical skin commensal but was selected for mechanistic reasons. Members of the *Corynebacterium* genus are relatively abundant components of the human skin microbiome [88,89], and have been associated with skin barrier function and aging-related parameters such as transepidermal water loss [90,91]. Moreover, microbiome studies in skin aging predominantly report alterations at the genus level, supporting genus-oriented approach in this study. Thus, *C. glutamicum* was used as a genetically tractable representative within the *Corynebacterium* genus to explore the selective modulation of Corynebacterium-related bacteria associated with aged skin. This experimental design represents a reductionist *in vitro* model rather than a direct replication of the *in vivo* skin ecosystem, and extrapolation to specific skin-associated *Corynebacterium* species requires confirmation in more complex microbiome or *ex vivo* skin models.

The observed microbial responses in this study were assessed based on differential growth patterns under controlled culture conditions, while physicochemical parameters were maintained according to standard protocols but not specifically evaluated. We also recognize that OD600 provides only a turbidity-based estimate of growth and does not distinguish viable cells or compositional shifts. In this study, it served as an initial screening tool, and future work is needed to incorporate colony-forming unit (CFU) enumeration and/or viability assays to better assess selective microbiome modulation. Thus, the selective modulation was interpreted within the established experimental framework. Further studies incorporating physicochemical analyses, such as pH and osmolarity, are needed to exclude non-specific growth effects and to distinguish direct microbial modulation from contributions of crude PP and PP.

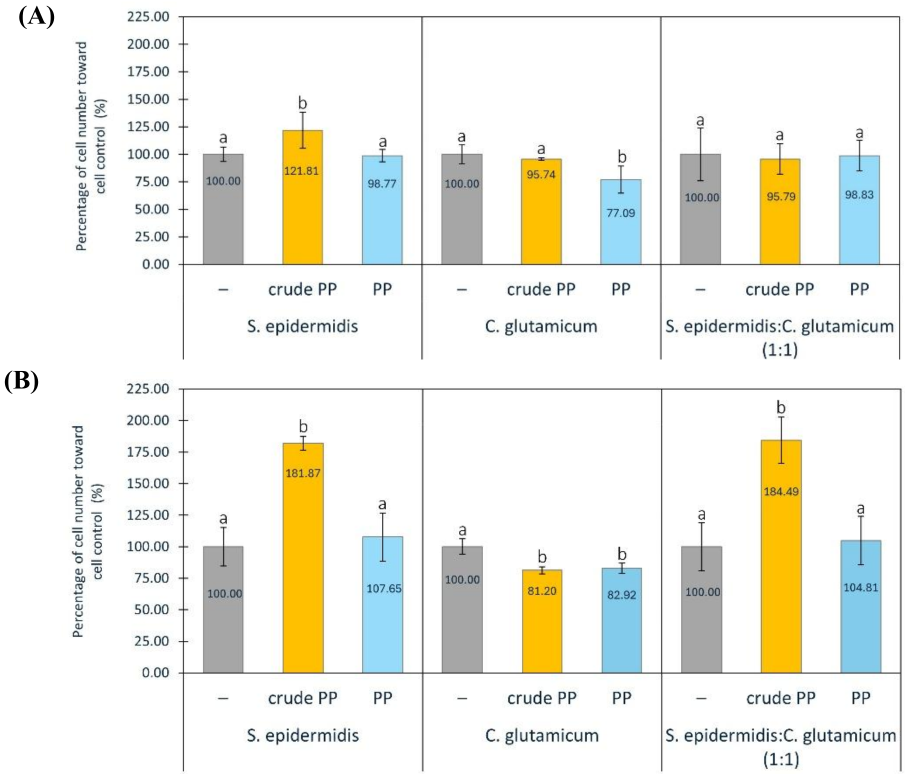

Figure 5 Percentage of *Staphylococcus epidermidis* and *Corynebacterium glutamicum* in monoculture and co-culture (1:1), without or with crude PP and PP at concentrations of 300 (A) and 600 µg/mL (B). Graph data are expressed as the mean of 3 replicates ± SD. Bar chart with different letter markers indicating significant differences ($p < 0.05$).

Analysis of peptide sequences and prediction of bioactive peptides

Overall, among the bioactive analyses of antioxidant, skin aging-related enzyme inhibition, cytoprotection, and microbial modulation, PP was more active than crude PP; therefore, the composition of peptides in PP was analyzed using the bottom-up proteomic approach. The completed LC-HRMS dataset, after analysis with SequestHT and the UniProt database, was provided as supplementary material. A total of 261 tryptic peptides were identified by LC-HRMS in the PP of BSFL. Based on the UniProt database, these tryptic peptides were derived from 142 BSFL proteins. Among the 261 tryptic peptides, 14 showed high PeptideRanker scores (> 0.60), indicating bioactivity (**Table 1**). The GRAVY scores of the tryptic peptides indicated that 4 peptides were relatively hydrophobic with GRAVY scores greater than 0, whereas the other ten peptides were more hydrophilic with GRAVY scores less than 0 (**Table 1**).

Table 1 Predictive bioactive tryptic peptides in pp by peptide ranker, and their properties.

No	Peptide sequence	Peptide ranker	Amino acid number	Molecular weight (Da)	Grant average of hydropathicity (GRAY)
1	DWWDDFDMPIR	0.943841	11	1,495.63	−1.155
2	AFQMFDPR	0.904916	8	1,011.16	−0.475
3	MSGFLWQR	0.900482	8	1,024.20	−0.200
4	ALQWIEAHPYKEEYANKPQRY	0.860472	21	2,634.90	−1.467
5	YVFLLFK	0.775047	7	929.15	1.743
6	SLEWNAAHPEEEREYIQGPGAAYK	0.77093	24	2,745.91	−1.204
7	EQFAALWR	0.757072	8	1,020.14	−0.275
8	AAPLLAAPAPIVAAR	0.720627	15	1,401.70	1.307
9	MSVVPLLFR	0.692318	9	1,061.34	1.533

No	Peptide sequence	Peptide ranker	Amino acid number	Molecular weight (Da)	Grant average of hydropathicity (GRAY)
10	FSEYFYPQIFAK	0.689513	12	1,539.72	−0.100
11	GQYSLIDADGFRR	0.618212	13	1,497.61	−0.731
12	AAPLVAAPVAAAAPVFAAR	0.612142	19	1,734.05	1.468
13	AEFKPYDHLR	0.601277	10	1,275.41	−1.310
14	LLDQHFGTGLR	0.60065	11	1,256.41	−0.182

Table 2 Total number of peptide targets, skin aging (SA)-related peptide targets, and the ratio of SA-related-peptide targets of predictive bioactive tryptic peptides.

No	Peptide sequence	Total number of SA-related peptide targets	Total number of peptide target	Ratio of SA-related peptide targets to total peptide targets	Ratio of SA- related peptide targets to total SA targets
1	DWWDDFDMPIR	36	166	0.217	0.042
2	AFQMFDPR	41	202	0.203	0.048
3	MSGFLWQR	41	228	0.180	0.048
4	ALQWIEAHPYKEEYANKPQRY	34	138	0.246	0.040
5	YVFLLFK	52	252	0.206	0.061
6	SLEWNAAHPEEEREYIQGPGAAYK	22	108	0.204	0.026
7	EQFAALWR	48	264	0.182	0.056
8	AAPLLAAPAPIVAAR	23	113	0.204	0.027
9	MSVVPLLFR	48	236	0.203	0.056
10	FSEYFYPQIFAK	42	198	0.212	0.049
11	GQYSLIDADGFRR	46	215	0.214	0.054
12	AAPLVAAPVAAAAPVFAAR	52	256	0.203	0.061
13	AEFKPYDHLR	40	190	0.211	0.047
14	LLDQHFGTGLR	40	203	0.197	0.047

Network pharmacology

Network pharmacology is a system-level approach that integrates computational and experimental data to map the complex interactions between bioactive compounds (including peptides), their molecular targets, and biological pathways [92]. It is important to acknowledge that the network pharmacology analysis conducted in this study is inherently dependent on publicly available databases and predictive algorithms. PeptideRanker predicts bioactivity based on machine-learning models trained on previously characterized peptides, potentially favoring sequence patterns that resemble known bioactive peptides [93]. Similarly, the Similarity Ensemble Approach (SEA) relies on chemical similarity to annotated ligands [94]. In addition, GeneCards integrates gene–disease associations from curated datasets, text mining, and literature-based evidence, which may overrepresent highly researched pathways such as proteolysis, apoptosis, and oxidative stress [95]. Consequently, hub proteins identified in this study may partly reflect database-driven research density. Therefore, the network pharmacology findings should be interpreted as hypothesis-generating, and require rigorous experimental validation to confirm direct molecular interactions and pathway modulation.

Based on the Similarity Ensemble Approach database in this study, 353 protein targets were predicted for 14 bioactive tryptic peptides. The targets for “skin aging” or “dysbiosis” (Skin Aging or SA) were 850 proteins, according to the Genecards database (**Figure 6(A)**). Among 353 proteins targeted by 14 bioactive tryptic peptides, 69 proteins were associated with skin aging, as shown in the intersection of the Venn diagram in **Figure 6(A)**. The bioactive tryptic peptides with the highest ratio of SA-related peptide targets to total SA targets were YVFLLFK and AAPLVAAPVAAAAP VFAAR (number 4 and 12 in **Table 2**), indicating that these 2 peptides may exhibit higher anti-premature aging activities, as they affect more target proteins related to skin aging than the other 12 tryptic peptides. ALQWIEAHPYKEEYANKPQRY had the highest ratio of SA-related peptide targets to total peptide targets (**Table 2**), indicating that this tryptic peptide targeted skin aging pathways more selectively than the other 13 tryptic peptides.

The 69 protein targets obtained from the intersection in **Figure 6(A)** were imported into the STRING database for PPI analysis and visualized using Cytoscape 3.10.4 software. Among the 69 proteins, 21 were retrieved by hub gene screening with a Degree between 3 and 49, Betweenness Centrality (BC) between 0.09 and 0.193, and Closeness Centrality (CC) between 0.495 and 0.792 (**Figure 6(C)**). The PPI network is shown in **Figures 6(B)** and **6(C)**; the larger the node, the darker the color, and the higher the centrality degree value of the node, implying more interactions of one node with others [96]. MMP9 (matrix metalloproteinase 9), STAT3 (signaling and transcription activation protein), CASP3 (caspase 3), and CD4 (T-cell surface glycoprotein CD4) nodes were larger, indicating that these targets may play a key role in skin aging.

To investigate the potential mechanisms of action of the 14 bioactive tryptic peptides in skin aging, GO pathway enrichment bubble maps were constructed (**Figure 7**). The protein targets were categorized into GO categories: Biological process (BP), cellular component (CC), and molecular function (MF). In the BP category, these targets were involved in biological processes such as proteolysis, extracellular organization, cellular response to ROS and UVA, cell proliferation and senescence, melanin biosynthesis, and defense response to bacteria. All BPs are hallmarks of skin aging. In the MF category, endopeptidase activity, specifically metalloendopeptidase and serine-type endopeptidase activities, was mainly involved. In the CC category, the extracellular matrix, extracellular space, cytosol, membrane, melanosome, and lysosome were mainly involved in biological processes.

Proteolysis, with the highest −log10 *p*-value in the BP category, correlated well with endopeptidase activity as the main MF category and extracellular matrix as the main CC category. MMP9, as the most central node in the PPI network, is suggested to be involved in this proteolysis process, specifically cleaving extracellular matrix gelatin types I and V, as well as collagens types IV and V [97]. In addition to MMP9, MMP1 and MMP2 were among the top 21 central nodes in the PPI network. Our *in vitro* study on collagenase inhibition demonstrated that collagenase from *Clostridium histolyticum*, a metalloendopeptidase, was inhibited by PP and crude PP (**Figure 2(C)**). This inhibition by PP and crude PP may also occur with other metalloendopeptidases, including MMP9, MMP1, and MMP2. STAT3 is a protein involved in cell cycle regulation by inducing the expression of key genes that facilitate progression from the G1 to S phase, thereby promoting cell proliferation [98]. The ability of PP to induce fibroblast proliferation was demonstrated in this in vitro study (**Figure 4**). Moreover, the cellular response to ROS was demonstrated by the activity of PP in protecting cells from mortality caused by hydrogen peroxide (**Figure 3**). The cytoprotective effect of PP may be linked to the inhibition of the cytosolic CASP3 node, which acts as a major effector caspase involved in the execution phase of apoptosis [99]. Tyrosinase (TYR) is also a target of bioactive tryptic peptides in PP, as shown in the PPI in **Figure 6(B)**, even though it is not included in the top 21 centrality nodes. The in vitro anti-tyrosinase activity of PP in this study may support the involvement of tyrosinase as a node target in the PPI network and melanosomes as a CC category. Dysbiosis, a hallmark of skin aging, is related to the biological process of defense responses to bacteria, as indicated by the BP of the GO category. The decrease in *Corynebacterium* abundance by PP and crude PP may be related to the BP of the bioactive tryptic peptide in the defense response to bacteria.

Some experimental evaluations in thus study were conducted using cell-free systems that do not fully recapitulate the complexity of intracellular signaling networks and tissue microenvironments. Therefore, while the current results may indicate potential protein target associations, they do not confirm direct modulation of these proteins by PP. Further validation in relevant cellular or aged tissue models is essential to substantiate the mechanistic involvement of MMP9, STAT3, and CASP3, including assessments at the gene and protein expression levels, activation status, and functional downstream effects.

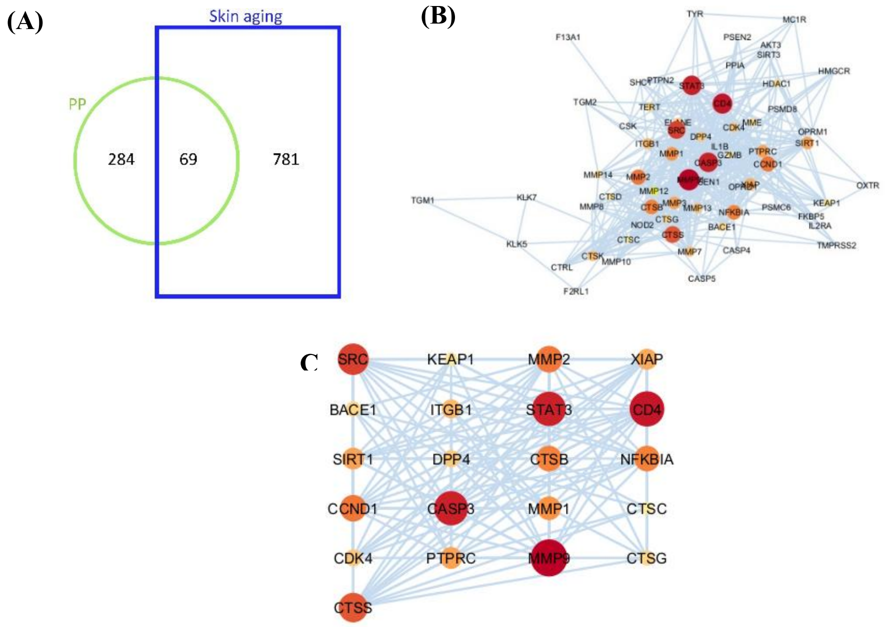

Figure 6 Network of PP bioactive tryptic peptide-target and skin aging target. (A) Common targets of predicted bioactive tryptic peptides and skin aging. (B) PPI network of intersection targets (69 targets) of bioactive tryptic peptides and skin aging. (C) PPI network of potential targets (21 targets) of bioactive tryptic peptides and skin aging after hub gene screening (Degree, BC, CC). The darker the color, the larger the node, the greater its degree value in the network, and the more important it is within the network.

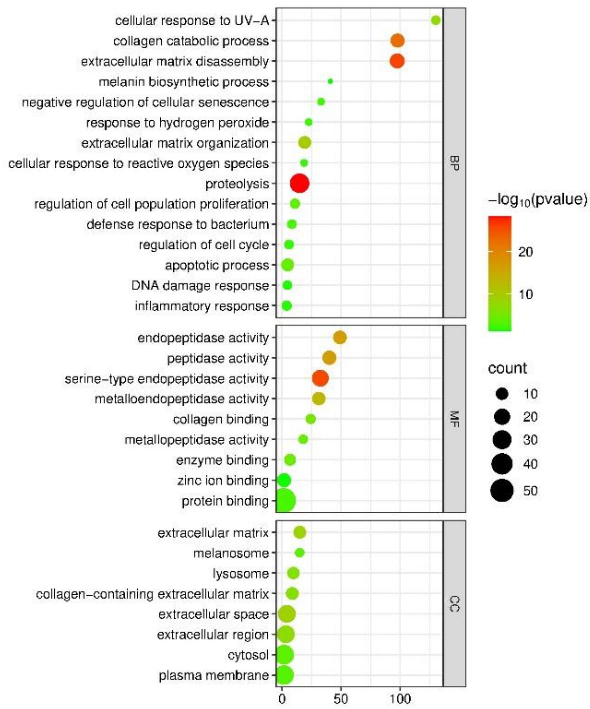

Figure 7 Enrichment analysis of intersection targets (67 targets) of PP bioactive tryptic peptide and skin aging. GO pathways are categorized into BP, MF and CC, and represent in bubble plot diagram according to –log *p* value, number of targets (count) and enrichment.

By integrating in vitro assay results with predicted target proteins, this study proposes mechanistic pathways wherein reactive oxygen species (ROS) serve as central mediators of premature skin aging (**Figure 8**). This occurs through the coupling of oxidative stress with melanogenesis, extracellular matrix (ECM) degradation, fibroblast loss, and microbial dysbiosis. Free radicals activate the Microphthalmia-Inducing Transcription Factor (MITF), leading to upregulation of tyrosinase expression and activity, which, in turn, increases melanin synthesis and clinical hyperpigmentation [8,100,101]. In dermal fibroblasts, oxidative stress upregulates and activates matrix metalloproteinases (MMPs) such as MMP-1, MMP-2, MMP-3, MMP-9, and MMP-13, leading to degradation of fibrillar collagen and other ECM components, causing skin wrinkles and sagging[102,103]. Beyond ECM degradation, ROS contributes to dermal atrophy by impairing fibroblast homeostasis. Oxidative stress can inhibit pro-survival signaling—including JAK/STAT3—and activate intrinsic apoptotic cascades, culminating in caspase-3 (CASP3) activation and reduced fibroblast number [104,105]. Reduced fibroblast viability directly translates into diminished collagen synthesis and exacerbates clinical signs of wrinkles and sagging [106].

Consistent with these mechanisms, several bioactive peptides have been reported to exert multi-target anti-skin-aging effects. For example, the cyclic peptide CR5 (CYGSR) shows strong antioxidant activity, almost complete tyrosinase inhibition, and marked MMP-1 suppression while enhancing type I procollagen, highlighting combined antioxidant, anti-tyrosinase, and anti-collagenase/ECM-protective actions [107]. Likewise, antioxidant peptides from Volvariella volvacea (e.g., DWPGFK) protect human skin fibroblasts from H_2O_2-induced oxidative damage, enhance antioxidant enzyme activity, and inhibit MMP activity, thereby limiting collagen degradation and supporting fibroblast survival [108]. These examples support the rationale for developing multifunctional peptides that integrate antioxidant, anti-melanogenic, anti-collagenase, and cytoprotective activities, in line with the pleiotropic profile observed for proteins and peptides from BSFL in this study.

The present findings showed that PP from BSFL counteracts the processes by inhibiting the oxidation reaction, inhibiting the activity of tyrosinase and collagenase, and also maintaining cell proliferation under oxidative stress conditions. Crude PP also has similar activities to PP, but without cytoprotection activity. In addition, growing evidence links skin aging to microbiome dysbiosis, with shifts in *Corynebacterium* and *Staphylococcus* associated with impaired barrier function and reduced hydration. By modulating these microbial genera, PP and crude PP may add a microbiome-mediated mechanism to their direct antioxidant, anti-melanogenic, and anti-wrinkle activities, positioning PP as a multi-target candidate for preventing ROS-driven hyperpigmentation and structural skin aging.

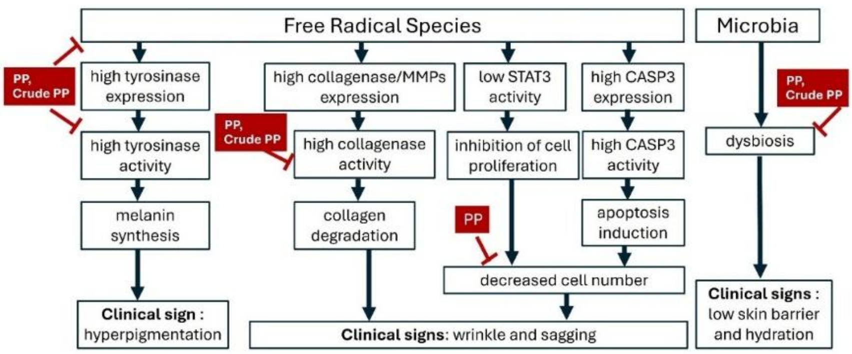

Figure 8 Proposed mechanistic pathways underlying premature skin aging induced by free radical species and microbial dysbiosis, and the modulatory effects of PP and crude PP from BSFL. The scheme integrates in vitro findings (antioxidant, anti-tyrosinase, anti-collagenase, cytoprotection, and microbial modulation) with network pharmacology-predicted targets (e.g., MMPs, STAT3, CASP3), highlighting potential molecular mechanisms leading to hyperpigmentation, wrinkle formation, sagging, and impaired skin barrier function.

The experimental evaluations in this study were conducted using in vitro and some using cell-free systems that do not fully recapitulate the complexity of intracellular signaling networks and tissue microenvironments. Therefore, while the current results may indicate potential protein targets (MMP9, STAT3 and CASP3), they do not confirm direct modulation of these proteins by PP. Further validation in relevant cellular or aged tissue models is essential to substantiate the mechanistic involvement of MMP9, STAT3, and CASP3, including assessments at the gene and protein expression levels, activation status, and functional downstream effects.

Conclusions

This study provides an integrated in vitro screening-level evaluation of protein and peptides derived from *Hermetia illucens* L. larvae in relation to pathways associated with premature skin aging. The protein and peptide fraction 3-30 kDa (PP) exhibited antioxidant activity, tyrosinase and collagenase inhibition, protection of NIH/3T3 fibroblasts under oxidative stress, and selective modulation of *Corynebacterium* and *Staphylococcus*-related bacterial growth in simplified culture systems. LC-HRMS identified 261 tryptic peptides, of which 14 were predicted to be bioactive, and network pharmacology suggested potential interactions with skin-aging–related targets, including MMP9, STAT3, and CASP3. Mechanistically, these findings indicate that PP may influence interconnected processes, including oxidative stress regulation, extracellular matrix remodeling, melanogenesis-related enzyme activity, and proliferation-associated signaling. Accordingly, the present findings establish a foundation for further validation in human skin models and mechanistic studies.

Acknowledgements

We acknowledge the Ministry of Research and Technology, Republic of Indonesia, for providing financial support for this research through the Fundamental Research Project 2025 scheme (Number: 0498.05/LL5-INT/AL.04/2025, 211/LPPM-Pen/In). We also sincerely thank Lorenza Feby Valentina Mardani, Dian Natalia Nainggolan, Stephanie, Delvira Sari, and Fabiana Disa for their technical support and lab management.

Declaration of generative AI in scientific writing

The authors acknowledge the use of generative AI tools (e.g., Paperpal by OpenAI) in the preparation of this manuscript, specifically for language editing and grammar correction. No content generation or data interpretation was performed by AI. The authors take full responsibility for the content and conclusions of this work

CRediT author statement

Sendy Junedi: Conceptualization; Methodology, Formal Analysis, Writing - Original Draft. **Boy Rahardjo Sidharta**: Investigation, Validation, Data curation. **Agustina Setiawati**: Investigation, Validation, Visualization. **Rudy Agung Nugroho**: Writing - Review & Editing.

References

[1] C Parrado, S Mercado-Saenz, A Perez-Davo, Y Gilaberte, S Gonzalez and A Juarranz. Environmental stressors on skin aging. Mechanistic Insights. *Frontiers in Pharmacology* 2019; **10**, 759.

[2] R Oizumi, Y Sugimoto and H Aibara. The Potential of exercise on lifestyle and skin function: Narrative review. *JMIR Dermatology* 2024; **7**, e51962.

[3] Z Peng, B Chen, Q Zheng, G Zhu, W Cao, X Qin and C Zhang. Ameliorative Effects of Peptides from the Oyster (*Crassostrea hongkongensis*) protein hydrolysates against UVB-induced skin photodamage in mice. *Marine Drugs* 2020; **18(6)**, 288.

[4] HR Kim, DH Jeong, S Kim, SW Lee, HS Sin, KY Yu, SI Jeong and SY Kim. Fermentation of blackberry with *L. plantarum* JBMI F5 enhance the protection effect on UVB-mediated photoaging in human foreskin fibroblast and hairless mice through regulation of MAPK/NF-κB signaling. *Nutrients* 2019; **11(10)**, 2429.

[5] HS Han, JS Shin, DB Myung, HS Ahn, SH Lee, HJ Kim and KT Lee. *Hydrangea serrata* (Thunb.) Ser. extract attenuate UVB-induced photoaging

through MAPK/AP-1 inactivation in human skin fibroblasts and hairless mice. *Nutrients* 2019; **11(3)**, 533.

[6] A Darawsha, A Trachtenberg, J Levy and Y Sharoni. The protective effect of carotenoids, polyphenols, and estradiol on dermal fibroblasts under oxidative stress. *Antioxidants* 2021; **10(12)**, 2023.

[7] JH Kim, HD Jeong, MJ Song, DH Lee, JH Chung and ST Lee. SOD3 suppresses the expression of MMP-1 and increases the integrity of extracellular matrix in fibroblasts. *Antioxidants* 2022; **11(5)**, 928.

[8] Y Wang, MM Hao, Y Sun, LF Wang, H Wang, YJ Zhang, HY Li, PW Zhuang and Z Yang. Synergistic promotion on tyrosinase inhibition by antioxidants. *Molecules* 2018; **23(1)**, 106.

[9] S Katiyar, D Yadav and SK Singh. Markers of oxidative stress and tyrosinase activity in melasma patients: A biochemical investigation. *Current Protein and Peptide Science* 2024; **25(2)**, 183-188.

[10] R Jugé, P Rouaud-Tinguely, J Breugnot, K Servaes, C Grimaldi, MP Roth, H Coppin and B Closs. Shift in skin microbiota of Western European women across aging. *Journal of Applied Microbiology* 2018; **125(3)**, 907-916.

[11] MHY Leung, D Wilkins and PKH Lee. Insights into the pan-microbiome: Skin microbial communities of Chinese individuals differ from other racial groups. *Scientific Reports* 2015; **5(1)**, 11845.

[12] B Howard, CC Bascom, P Hu, RL Binder, G Fadayel, TG Huggins, BB Jarrold, R Osborne, HL Rocchetta, D Swift, JP tiesman, Y Song, Y Wang, K wehmeyer, AB Kimball and RJ Isfort. Aging-associated changes in the adult human skin microbiome and the host factors that affect skin microbiome composition. *Journal of Investigative Dermatology* 2022; **142(7)**, 1934-1946.

[13] C Sun, G Hu, L Yi, W Ge, Q Yang, X Yang, Y He, Z Liyu and WH Chen. Integrated analysis of facial microbiome and skin physio-optical properties unveils cutotype-dependent aging effects. *Microbiome* 2024; **12(1)**, 163.

[14] Y Jung, I Kim, DR Jung, JH Ha, EK Lee, JM Kim, JY kim, JH Jang, JT Bae, JH Shin and YS Cho. Aging-induced changes in cutibacterium acnes and their effects on skin elasticity and wrinkle formation. *Microorganisms* 2024; **12(11)**, 2179.

[15] S Iglesia, T Kononov and AS Zahr. A multi-functional anti-aging moisturizer maintains a diverse and balanced facial skin microbiome. *Journal of Applied Microbiology* 2022; **133(3)**, 1791-1799.

[16] F Mei, J Liu, J Wu, Z Duan, M Chen, K Meng, S Chen, X Shen, G Xia and M Zhao. Collagen peptides isolated from salmo salar and tilapia nilotica skin accelerate wound healing by altering cutaneous microbiome colonization via upregulated NOD2 and BD14. *Journal of Agricultural and Food Chemistry* 2020; **68(6)**, 1621-1633.

[17] J Mu, Q Lin, S Wang, M Chen, J Wang, Y Chen, Y Li and Y Liang. TNF-α modulation by rice bran peptides: Implications for gut microbiota stability and cognitive health in aging. *Npj Biofilms and Microbiomes* 2025; **11(1)**, 195.

[18] MG Claros, M Lequio, S Cheli, AB Garlatti, N Cecilia, L Juarez, M Bittar, MJ Leiva, ML Hernandez, JM Márquez, G Babaracco and SL Mercier. A cross-sectional epidemiological study conducted in Argentina to evaluate the impact of the exposome on skin aging. *Journal of Cosmetic Dermatology* 2023; **22(12)**, 3459-3469.

[19] JY Ng, H Zhou, T Li and FT Chew. Comparisons between wrinkles and photo-ageing detected and self-reported by the participant or identified by trained assessors reveal insights from Chinese individuals in the Singapore/Malaysia Cross-sectional Genetics Epidemiology Study (SMCGES) cohort. *Journal of Physiological Anthropology* 2024; **43(1)**, 14.

[20] AC Green, MCB Hughes, P McBridea and A Fourtanier. Factors Associated with premature skin aging (photoaging) before the age of 55: A population-based study. *Dermatology* 2011; **222(1)**, 74-80.

[21] SH Zyoud, T Ahmada nd SW Al-Jabi. Mapping the global research landscape: A bibliometric analysis of clinical trials on skin aging - trends, innovations, and research gaps. *Aesthetic Plastic Surgery* 2025; **49(17)**, 5055-5058.

[22] R Tenchov, JM Sasso, X Wang and QA Zhou. Antiaging strategies and remedies: A landscape of

research progress and promise. *ACS Chemical Neuroscience* 2024; **15(3)**, 408-446.

[23] M Lau, J Mineroff Gollogly, JY Wang and J Jagdeo. Cosmeceuticals for antiaging: A systematic review of safety and efficacy. *Archives of Dermatological Research* 2024; **316(5)**, 173.

[24] PLM Alves, V Nieri, F de C Moreli, E Constantino, J de Souza, Y Oshima-Franco and D Grotto. Unveiling New horizons: Advancing technologies in cosmeceuticals for anti-aging solutions. *Molecules* 2024; **29(20)**, 4890.

[25] W Klinngam, A Chaiwichien, S Osotprasit, U Ruktanonchai, M Kanlayavattanakul, N Lourith, A Wongrakpanich, V Teeranachaideekul and T Iempridee. Longevity cosmeceuticals as the next frontier in cosmetic innovation: a scientific framework for substantiating product claims. *Frontiers in Aging* 2025; **6**, 1586999.

[26] M Tomas, D Günal-Köroğlu, S Kamiloglu, T Ozdal and E Capanoglu. The state of the art in anti-aging: Plant-based phytochemicals for skin care. *Immunity & Ageing* 2025; **22(1)**, 5.

[27] H Wang, J Zheng, S Cao and J Lv. Research on the mechanisms of plant bioactive metabolites in anti-skin aging and future development prospects. *Frontiers in Pharmacology* 2025; **16**, 1673075.

[28] JE Aguilar-Toalá, A Hernández-Mendoza, AF González-Córdova, B Vallejo-Cordoba and AM Liceaga. Potential role of natural bioactive peptides for development of cosmeceutical skin products. *Peptides* 2019; **122**, 170170.

[29] A Pintea, A Manea, C Pintea, RA Vlad, M Bîrsan, P Antonoaea, EM Rédai and A Ciurba. Peptides: Emerging candidates for the prevention and treatment of skin senescence: A review. *Biomolecules* 2025; **15(1)**, 88.

[30] MS Ferreira, MC Magalhães, JM Sousa-Lobo and IF Almeida. Trending anti-aging peptides. *Cosmetics* 2020; **7(4)**, **91**

[31] Z Xia, W Liu, F Zeng, S Kang, J Li, W Xu, P Tang, X Zheng, D Li, X Yang, Q Sheng and X Li. Systematic evaluation and identification of anti-inflammatory and anti-aging ginseng peptides for skincare applications. *Cosmetics* 2025; **12(2)**, 85.

[32] SA Siddiqui, B Ristow, T Rahayu, NS Putra, NW Yuwono, K Nisa, B Mategako, S Smetana, M Saki, A Nawaz and A Nagdalian. Black soldier fly larvae (BSFL) and their affinity for organic waste processing. *Waste Management* 2022; **140**, 1-13.

[33] S Ebeneezar, D Linga Prabu, CS Tejpal, NS Jeena, R Summaya, S Chandrasekar, P Sayooj and P Vijayagopal. Nutritional evaluation, bioconversion performance and phylogenetic assessment of black soldier fly (*Hermetia illucens,* Linn. 1758) larvae valorized from food waste. *Environmental Technology & Innovation* 2021; **23**, 101783.

[34] Saputra and YN Lee. Nutrition composition of commercial full-fat and defatted black soldier fly larvae meal (*Hermetia illucens*) as a potential protein resource for aquafeeds. *Biodiversitas* 2023; **24(9)**, 4877-4884.

[35] JA Khan, X Guo, R Pichner, K Aganovic, V Heinz, C Hollah, SV Miert, GR Verheyan, A Juadjur and KU Rehman. Evaluation of nutritional and techno-functional aspects of black soldier fly high-protein extracts in different developmental stages. *Animal* 2025; **19(4)**, 101463.

[36] J Lu, Y Guo, A Muhmood, B Zeng, Y Qiu, P Wang and L Ren. Probing the antioxidant activity of functional proteins and bioactive peptides in Hermetia illucens larvae fed with food wastes. *Scientific Reports* 2022; **12(1)**, 2799.

[37] M Firmansyah and MY Abduh. Production of protein hydrolysate containing antioxidant activity from *Hermetia illucens*. *Heliyon* 2019; **5(6)**, e02005.

[38] SI Park, JW Kim and SM Yoe. Purification and characterization of a novel antibacterial peptide from black soldier fly (*Hermetia illucens*) larvae. *Developmental and Comparative Immunology* 2015; **52(1)**, 98-106.

[39] T Pimchan, A Hamzeh, P Siringan, K Thumanu, Y Hanboonsong and J Yongsawatdigul. Antibacterial peptides from black soldier fly (*Hermetia illucens*) larvae: Mode of action and characterization. *Scientific Reports* 2024; **14(1)**, 26469.

[40] DH Lee, KB Chu, HJ Kang, SH Lee and FS Quan. Peptides in the hemolymph of *Hermetia illucens* larvae completely inhibit the growth of *Klebsiella pneumonia in vitro* and *in vivo*. *Journal of Asia-Pacific Entomology* 2020; **23(1)**, 36-43.

[41] SI Park and SM Yoe. Defensin-like peptide3 from black soldier fly: Identification, characterization, and key amino acids for anti-Gram-negative bacteria. *Entomological Research* 2017; **47(1)**, 41-47.

[42] X Xiaoyan, S Hongxia, G Jiamin, C Huicheng, L Ye and X Qiang. Antimicrobial peptide HI-3 from *Hermetia illucens* alleviates inflammation in lipopolysaccharide-stimulated RAW264.7 cells via suppression of the nuclear factor kappa-B signaling pathway. Microbiology and Immunology 2023; **67(1)**, 32-43.

[43] D Sandakila, GD Hadi, R Gultom, S Samalele and RA Nugroho. Ethanolic extract of black soldier fly (*Hermetia illucens* L.) larvae for wound healing in mice (*Mus musculus* L.). *Aceh Journal of Animal Science* 2024; **9(3)**, 119-127.

[44] CS Wu, SS Wang, DY Wu and W Gu. Modified poly(ε-caprolactone) with larvae protein environmentally friendly nanofiber: Assessment of interface properties and characterization. *Express Polymer Letters* 2024; **18(8)**, 835-850.

[45] VA Duong and H Lee. Bottom-up proteomics: Advancements in sample preparation. *International Journal of Molecular Sciences* 2023; **24(6)**, 5350.

[46] T Puopolo, NP Seeram and C Liu. Chloroform/methanol protein extraction and in-solution trypsin digestion protocol for bottom-up proteomics analysis. *Bio-Protocol* 2024; **14(16)**, e5055.

[47] JM Burkhart, C Schumbrutzki, S Wortelkamp, A Sickmann and RP Zahedi. Systematic and quantitative comparison of digest efficiency and specificity reveals the impact of trypsin quality on MS-based proteomics. *Journal of Proteomics* 2012; **75(4)**, 1454-1462.

[48] JV Olsen, SE Ong and M Mann. Trypsin cleaves exclusively c-terminal to arginine and lysine residues. *Molecular & Cellular Proteomics* 2004; **3(6)**, 608-614.

[49] S Sedláčková, M Hubálek, V Vrkoslav, M Blechová, P Kozlík and J Cvačka. Positive effect of acetylation on proteomic analysis based on liquid chromatography with atmospheric pressure chemical ionization and photoionization mass spectrometry. *Molecules* 2023; **28(9)**, 3711.

[50] MS Mansuri, S Bathla, TT Lam, AC Nairn and KR Williams. Optimal conditions for carrying out trypsin digestions on complex proteomes: From bulk samples to single cells. *Journal of Proteomics* 2024; **297**, 105109.

[51] D Purcell, MA Packer and M Hayes. Identification of bioactive peptides from a laminaria digitata protein hydrolysate using *in silico* and *in vitro* methods to identify angiotensin-1-converting enzyme (ACE-1) Inhibitory peptides. *Marine Drugs* 2023; **21(2)**, 90.

[52] ER Coscueta, P Batista, JEG Gomes, R da Silva and MM Pintado. Screening of novel bioactive peptides from goat casein: *In silico* to *in vitro* validation. *International Journal of Molecular Sciences* 2022; **23(5)**, 2439.

[53] D Szklarczyk, K Nastou, M Koutrouli, R Kirsch, F Mehryary, R Hachilif, D Hu, ME Peluso, Q Huang, T Fang, NT Doncheva, S Pyysalo, P Bork, LJ Jensen and CV Mering. The STRING database in 2025: Protein networks with directionality of regulation. *Nucleic Acids Research* 2025; **53(D1)**, D730-D737.

[54] RA Nugroho, R Aryani, EH Hardi, H Manurung, R Rudianto and WN Jati. Fermented palm kernel waste with different sugars as substrate for black soldier fly larvae. *Global Journal of Environmental Science and Management* 2024; **10(2)**, 503-516.

[55] B Hoc, G Noël, J Carpentier, F Francis and RC Megido. Optimization of black soldier fly (*Hermetia illucens*) artificial reproduction. *Plos One* 2019; **14(4)**, e0216160.

[56] R Aryani, R Rosnadia, I Irma, H Manurung, R Rudianto and R Nugroho. Biochemical and immune modulation in mice fed defatted black soldier fly (*Hermetia illucens* L.) larvae meal. *Tropical Journal of Natural Product Research* 2025; **9(7)**, 3067-3075.

[57] JH Xu, S Xiao, JH Wang, B Wang, YX Cai and WF Hu. Comparative study of the effects of ultrasound-assisted alkaline extraction on black soldier fly (*Hermetia illucens*) larvae protein: Nutritional, structural, and functional properties. *Ultrasonics Sonochemistry* 2023; **101**, 106662.

[58] F Namjoyan, A Jahangiri, ME Azemi and H Mousavi. Inhibitory effects of *Urginea maritima*

(L.) baker, *Zhumeria majdae* Rech. F. and Wendelbo and *Physalis divaricata* D. Don ethanolic extracts on mushroom tyrosinase. *Pharmaceutical Sciences* 2016; **22(2)**, 81-86.

[59] S Sen, S Ghosh, S De, P Basak, P Maurye, NK Jana and TK Mandal. Immunomodulatory and antimicrobial non-mulberry Antheraea mylitta silk fibroin accelerates *in vitro* fibroblast repair and regeneration by protecting oxidative stress. *RSC Advances* 2021; **11(31)**, 19265-19282.

[60] H Ardalani, S Anam, KJK Kromphardt, D Staerk and KT Kongstad. Coupling microplate-based antibacterial assay with liquid chromatography for high-resolution growth inhibition profiling of crude extracts: Validation and proof-of-concept study with *Staphylococcus aureus*. *Molecules* 2021; **26(6)**, 1550.

[61] K Praseatsook, A Vachiraarunwong, S Taya, P Setthaya, K Sato, H Wanibuchi, R Wongpoomchai, P Dejkriengkraikul, M Gi and S Yodkeree. Anticancer and antioxidant effects of bioactive peptides from black soldier fly larvae (*Hermetia illucens*). *Nutrients* 2025; **17(4)**, 645.

[62] J Pan, H Xu, M Dabbour, B Kumah Mintah, W Chen, F Yang, Z Zhang, Y Cheng, C Dai, R He and H Ma. Effect of alkaline pH-shifting process on extraction rate, structural, and functional properties of black soldier fly (*Hermetia illucens*) larvae protein. *LWT* 2023; **185**, 115180.

[63] L Miron, G Montevecchi, G Bruggeman, LI Macavei, L Maistrello, A Antonelli and M Thomas. Functional properties and essential amino acid composition of proteins extracted from black soldier fly larvae reared on canteen leftovers. *Innovative Food Science and Emerging Technologies* 2023; **87**, 103407.

[64] B Zozo, M Wicht and J van Wyk. Effect of alkaline extraction-isoelectric precipitation and salt-assisted extraction on physicochemical and techno-functional properties of black soldier fly larvae proteins. *Applied Sciences* 2024; **14(24)**, 11485.

[65] Z Chang, B Fu, M Li, S Cheng and M Du. Advancements in identification of low-molecular-weight peptides in food protein hydrolysates. *Food Frontiers* 2025; **6(5)**, 2144-2164.

[66] N Landi, A Clemente, PV Pedone, S Ragucci and A Di Maro. An updated review of bioactive peptides from mushrooms in a well-defined molecular weight range. *Toxins* 2022; **14(2)**, 84.

[67] D Zhu, X Huang, F Tu, C Wang and F Yang. Preparation, antioxidant activity evaluation, and identification of antioxidant peptide from black soldier fly (*Hermetia illucens* L.) larvae. *Journal of Food Biochemistry* 2020; **44(5)**, e13186.

[68] L Meng, D Yu, J Lin, Y Hu, N Peng and S Zhao. Structural characterization, HepG2 cell cytoprotective ability, and antioxidant mechanism of novel antioxidant peptides identified from black soldier fly larvae (*Hermetia illucens* L.). *Food Chemistry* 2025; **463**, 141462.

[69] MP Germanò, F Cacciola, P Donato, P Dugo, G Certo, V D'Angelo, L Mondello and A Rapisarda. Betula pendula leaves: Polyphenolic characterization and potential innovative use in skin whitening products. *Fitoterapia* 2012; **83(5)**, 877-882.

[70] B Gąsowska-Bajger and H Wojtasek. Epigallocatechin and epigallocatechin-3-gallate are not inhibitors of tyrosinase. *Bioorganic & Medicinal Chemistry Letters* 2024; **113**, 129976.

[71] I Kubo, QX Chen and K Nihei. Molecular design of antibrowning agents: Antioxidative tyrosinase inhibitors. *Food Chemistry* 2023; **81(2)**, 241-247.

[72] M Taheri, F Seirafianpour, A Fallahian, A Hosseinzadeh, RJ Reiter and S Mehrzadi. Exploring melatonin's signalling pathways in the protection against age-related skin deterioration. *Pharmacological Reports* 2025; **77(2)**, 375-391.

[73] S Lee, BH Kim, YJ Choi, DW Kim, E Cho, M Kang, D Kim, J Pyo and KS Kang. Inhibition of TNF-α-induced collagen degradation and oxidative damage by *Centipeda minima* and Brevilin A in human dermal fibroblasts. *Current Issues in Molecular Biology* 2025; **47(5)**, 376.

[74] S Pientaweeratch, V Panapisal and A Tansirikongkol. Antioxidant, anti-collagenase and anti-elastase activities of *Phyllanthus emblica*, *Manilkara zapota* and silymarin: An *in vitro* comparative study for anti-aging applications. *Pharmaceutical Biology* 2016; **54(9)**, 1865-1872.

[75] YC Loo, HC Hu, SY Yu, YH Tsai, M Korinek, YC Wu, FR Chang and YJ Chen. Development on

potential skin anti-aging agents of *Cosmos caudatus* Kunth via inhibition of collagenase, MMP-1 and MMP-3 activities. *Phytomedicine* 2023; **110**,154643.

[76] W Xue, X Liu, X., W Zhao and Z Yu. Identification and molecular mechanism of novel tyrosinase inhibitory peptides from collagen. *Journal of Food Science* 2022; **87(6)**, 2744-2756.

[77] M Dymek, D Warszycki, S Podlewska and E Sikora. Novel tripeptides as tyrosinase inhibitors: *In silico* and *in vitro* approaches. *International Journal of Molecular Sciences* 2024; **25(24)**, 13509.

[78] PG Yap and CY Gan. Multifunctional tyrosinase inhibitor peptides with copper chelating, UV-absorption and antioxidant activities: Kinetic and docking studies. *Foods* 2021; **10(3)**, 675.

[79] A Sargsyan, H Hakobyan, Z Mardiyan, S Jamharyan, A Dadayan, T Sargsyan and N Hovhannisyan. Modeling, synthesis and *in vitro* screening of unusual amino acids and peptides as protease inhibitors. *Journal of Chemical Technology and Metallurgy* 2023; **58(3)**, 615-620.

[80] GR Rama, LFSM Timmers and CFV de Souza. *In silico* strategies to predict anti-aging features of whey peptides. *Molecular Biotechnology* 2024; **66(9)**, 2426-2440.

[81] K Yeerong, P Chantawannakul, S Anuchapreeda, S Wangtueai and W Chaiyana. Optimization of hydrolysis conditions, isolation, and identification of biologically active peptides derived from acheta domesticus for antioxidant and collagenase inhibition. *Antioxidants* 2024; **13(3)**, 367.

[82] N Talachi, E Afzal, M Nouri, S Abroun, M Zarrabi and H Jahandar. Protective effect of human amniotic membrane extract against hydrogen peroxide-induced oxidative damage in human dermal fibroblasts. *International Journal of Cosmetic Science* 2023; **45(1)**, 73-82.

[83] N Zhu, R Liu, M Xu and Y Li. The potential of bioactive fish collagen oligopeptides against hydrogen peroxide-induced NIH/3T3 and HUVEC damage: The involvement of the mitochondria. *Nutrients* 2024; **16(7)**, 1004.

[84] N Zhu, MH Xu and Y Li. Bioactive oligopeptides from ginseng (*Panax ginseng* Meyer) suppress oxidative stress-induced senescence in fibroblasts via NAD+/SIRT1/PGC-1α signaling pathway. *Nutrients* 2022; **14(24)**, 5289.

[85] ME Giordano, F Lionetto and MG Lionetto. Impact of polyethylene terephthalate nanoplastics (PET) on fibroblasts: A study on NIH-3T3 cells. *Frontiers in Physiology* 2025; **16**, 1580682.

[86] P Branco, EM Maurício, A Costa, D Ventura, C Roma-Rodrigues, MP Duarte, AR Fernandes and C Prista. Exploring the multifaceted potential of a peptide fraction derived from *Saccharomyces cerevisiae* metabolism: Antimicrobial, antioxidant, antidiabetic, and anti-inflammatory properties. *Antibiotics* 2023; **12(8)**, 1332.

[87] B Masoumifeshani, AA Kenari, I Sottorff, M Crüsemann and JA Moghaddam. Identification and evaluation of antioxidant and anti-aging peptide fractions from enzymatically hydrolyzed proteins of *Spirulina platensis* and *Chlorella vulgaris*. *Marine Drugs* 2025; **23(4)**, 162.

[88] R Herman, S Meaden, M Rudden, R Cornmell, HN Wilkinson, MJ Hardman, AJ Wilkinson, B Murphy and GH Thomas. Revealing the diversity of commensal corynebacteria from a single human skin site. *mSystems* 2025; **10(10)**, e00459-25.

[89] MG Jensen, L Svraka, E Baez, M Lund, A Poehlein and H Brüggemann. Species- and strain-level diversity of *Corynebacteria* isolated from human facial skin. *BMC Microbiology* 2023; **23(1)**, 366.

[90] JH Kim, SM Son, H Park, BK Kim, IS Choi, H Kim and CS Huh. Taxonomic profiling of skin microbiome and correlation with clinical skin parameters in healthy Koreans. *Scientific Reports* 2021; **11(1)**, 16269.

[91] T Myers, A Bouslimani, S Huang, ST Hansen, C Clavaud, A Azouaoui, A Ott, A Gueniche, C Bouez, Q Zheng, L Aguilar, R Knight, M Moreau and SJ Song. A multi-study analysis enables identification of potential microbial features associated with skin aging signs. *Frontiers in Aging* 2024; **4**, 1304705.

[92] KY Hsin, S Ghosh and H Kitano. Combining machine learning systems and multiple docking simulation packages to improve docking prediction reliability for network pharmacology. *Plos One* 2013; **8(12)**, e83922.

[93] C Mooney, NJ Haslam, G Pollastri and DC Shields. Towards the improved discovery and design of functional peptides: Common features of diverse classes permit generalized prediction of bioactivity. *Plos One* 2012; **7(10)**, e45012.

[94] MJ Keiser, BL Roth, BN Armbruster, P Ernsberger, JJ Irwin and BK Shoichet. Relating protein pharmacology by ligand chemistry. *Nature Biotechnology* 2007; **25(2)**, 197-206.

[95] D Grissa, A Junge, TI Oprea and LJ Jensen. Diseases 2.0: A weekly updated database of disease-gene associations from text mining and data integration. *Database* 2022; **2022**, baac019.

[96] M Ashtiani, A Salehzadeh-Yazdi, Z Razaghi-Moghadam, H Hennig, O Wolkenhauer, M Mirzaie and M Jafari. A systematic survey of centrality measures for protein-protein interaction networks. *BMC Systems Biology* 2018; **12(1)**, 80.

[97] SR Van Doren. Matrix metalloproteinase interactions with collagen and elastin. *Matrix Biology* 2015; **44-46**, 224-231.

[98] T Shirogane, T Fukada, JMM Muller, DT Shima, M Hibi and T Hirano. Synergistic Roles for Pim-1 and c-Myc in STAT3-mediated cell cycle progression and antiapoptosis. *Immunity* 1999; **11(6)**, 709-719.

[99] S McComb, PK Chan, A Guinot, H Hartmannsdottir, S Jenni, MP Dobay, JP Bourquin and BC Bornhauser. Efficient apoptosis requires feedback amplification of upstream apoptotic signals by effector caspase-3 or -7. *Science Advances* 2019; **5(7)**, eaau9433.

[100] Y Song, S Chen, L Li, Y Zeng and X Hu. The hypopigmentation mechanism of tyrosinase inhibitory peptides derived from food proteins: An overview. *Molecules* 2022; **27(9)**, 2710.

[101] Y Lu, KF Tonissen and G Di Trapani. Modulating skin colour: Role of the thioredoxin and glutathione systems in regulating melanogenesis. *Bioscience Reports* 2021; **41(5)**, BSR20210427.

[102] D Pujimulyani, CL Suryani, A Setyowati, RAS Handayani, S Arumwardana, W Widowati and A Maruf. Cosmeceutical potentials of Curcuma mangga Val. extract in human BJ fibroblasts against MMP1, MMP3, and MMP13. *Heliyon* 2020; **6(9)**, e04921.

[103] W Choi, HS Kim, SH Park, D Kim, YD Hong, JH Kim and JY Cho. Syringaresinol derived from Panax ginseng berry attenuates oxidative stress-induced skin aging via autophagy. *Journal of Ginseng Research* 2022; **46(4)**, 536-542.

[104] T Tanigawa, S Kanazawa, R Ichibori, T Fujiwara, T Magome, K Shingaki, S Miyata, Y Hata, K Tomita, K Matsuda, T Kubo, M Tohyama, K Yano and K Hosokawa. (+)-Catechin protects dermal fibroblasts against oxidative stress-induced apoptosis. *BMC Complementary and Alternative Medicine* 2014; **14(1)**, 133.

[105] HJ Cho, JA Hwang, EJ Yang, EC Kim, JR Kim, SY Kim, YZ Kim, SC Park and YS Lee. Nintedanib induces senolytic effect via STAT3 inhibition. *Cell Death & Disease* 2022; **13(9)**, 760.

[106] J Zhang, H Yu, MQ Man and L Hu. Aging in the dermis: Fibroblast senescence and its significance. *Aging Cell* 2024; **23(2)**, e14054.

[107] GH Kim and BM Kim. *In vitro* and *in silico* evaluation of a novel multifunctional cyclic peptide with antioxidant, tyrosinase-inhibitory, and extracellular matrix-modulating activities. *International Journal of Molecular Sciences* 2025; **26(22)**, 10878.

[108] B Xu, Y Wang, L Zha, M Chen, P Yu, Q Dong, O Suwantong and Y Zhao. Novel antioxidant peptides from hydrolyzed proteins of *Volvariella volvacea*: Purification, characterization and protective effects on H_2O_2-induced human skin fibroblasts. *Food Bioscience* 2025; **64**, 105825.